THE JOURNAL OF BIOLOGICAL CHEMISTRY VOL. 291, NO. 20, pp. 10736–10746, May 13, 2016


# Staphylococcal Nuclease and Tudor Domain Containing 1 (SND1 Protein) Promotes Hepatocarcinogenesis by Inhibiting Monoglyceride Lipase (MGLL)*[S]

Received for publication, January 12, 2016, and in revised form, March 10, 2016 Published, JBC Papers in Press, March 20, 2016, DOI 10.1074/jbc.M116.715359

**Devaraja Rajasekaran[‡], Nidhi Jariwala[‡], Rachel G. Mendoza[‡], Chadia L. Robertson[‡1], Maaged A. Akiel[‡], Mikhail Dozmorov[§], Paul B. Fisher[‡¶‖2], and Devanand Sarkar[‡¶‖3]**

*From the Departments of [‡]Human and Molecular Genetics and [§]Biostatistics, [¶]Massey Cancer Center, and [‖]VCU Institute of Molecular Medicine, Virginia Commonwealth University, Richmond, Virginia 23298*

**Staphylococcal nuclease and tudor domain containing 1 (SND1) is overexpressed in multiple cancers, including hepatocellular carcinoma (HCC), and functions as an oncogene. This study was carried out to identify novel SND1-interacting proteins to better understand its molecular mechanism of action. SND1-interacting proteins were identified by a modified yeast two-hybrid assay. Protein-protein interaction was confirmed by co-immunoprecipitation analysis. Monoglyceride lipase (MGLL) expression was analyzed by quantitative RT-PCR, Western blot, and immunohistochemistry. MGLL-overexpressing clones were analyzed for cell proliferation and cell cycle analysis and *in vivo* tumorigenesis in nude mice. MGLL was identified as an SND1-interacting protein. Interaction of SND1 with MGLL resulted in ubiquitination and proteosomal degradation of MGLL. MGLL expression was detected in normal human hepatocytes and mouse liver, although it was undetected in human HCC cell lines. An inverse correlation between SND1 and MGLL levels was identified in a human HCC tissue microarray as well as in the TCGA database. Forced overexpression of MGLL in human HCC cells resulted in marked inhibition in cell proliferation with a significant delay in cell cycle progression and a marked decrease in tumor growth in nude mouse xenograft assays. MGLL overexpression inhibited Akt activation that is independent of enzymatic activity of MGLL and overexpression of a constitutively active Akt rescued cells from inhibition of proliferation and restored normal cell cycle progression. This study unravels a novel mechanism of SND1 function and identifies MGLL as a unique tumor suppressor for HCC. MGLL might function as a homeostatic regulator of Akt restraining its activation.**

Staphylococcal nuclease and tudor domain containing 1 (SND1) is a multifunctional protein regulating transcription, RNA interference (RNAi) and mRNA splicing, editing, and stability and functions as an oncogene in multiple cancers (1). SND1 overexpression has been observed in cancers of liver, colon, breast, brain, and prostate, and overexpression and knockdown studies have confirmed that SND1 promotes the hallmarks of cancer, such as proliferation, invasion, epithelial-mesenchymal transition, angiogenesis, and metastasis (2–8). As a pleiotropic protein, SND1 promotes tumorigenesis in multiple ways. We documented that SND1 promotes RNA-induced silencing complex activity in hepatocellular carcinoma (HCC)[4] cells thus facilitating oncogenic miRNA-mediated degradation of tumor suppressor mRNAs and thereby facilitating hepatocarcinogenesis (2). In HCC cells, SND1 promotes angiogenesis by activating a linear pathway involving NF-$\kappa$B, miRNA-221, angiogenin, and CXCL16, and it promotes epithelial-mesenchymal transition via angiotensin II type 1 receptor (AT1R) and TGF$\beta$ signaling pathway (7, 8). Studies in breast cancer cells have identified SND1 as a downstream target of TGF$\beta$ signaling where it promotes metastasis by increasing E3 ubiquitin ligase Smurf1 leading to RhoA ubiquitination and degradation (9). Additionally SND1 is required for expansion and activity of tumor-initiating cells in the breast cancer model (6). In colon cancer cells, SND1 promotes tumorigenesis by activating Wnt/$\beta$-catenin pathway (4). SND1 functions as an anti-apoptotic protein, and cleavage of SND1 by caspases is necessary during drug-induced apoptosis (10). These findings indicate that SND1 promotes tumorigenesis by diverse mechanisms, and more in-depth studies are necessary to better understand the molecular mechanisms by which SND1 exerts its oncogenic function.

Triglycerides are broken down into fatty acids and glycerol by sequential action of multiple enzymes (11). Triglyceride lipase breaks down triglyceride into diacylglycerols, which are further broken down to monoacylglycerols by hormone-sensitive lipase. Monoglyceride lipase (MGLL) finally breaks down

* This work was supported in part by The James S. McDonnell Foundation, NCI Grants R01 CA138540 and R21 CA183954 (to D. S.) and R01 CA134721 (to P. B. F.) from National Institutes of Health, and the National Foundation for Cancer Research (to P. B. F.). The authors declare that they have no conflicts of interest with the contents of this article. The content is solely the responsibility of the authors and does not necessarily represent the official views of the National Institutes of Health.

[S] This article contains supplemental Table S1.

[1] Supported by NIDDK Grant T32DK007150 from National Institutes of Health.

[2] Holds the Thelma Newmeyer Corman Chair in Cancer Research and is a Samuel Waxman Cancer Research Foundation Investigator.

[3] Harrison Endowed Scholar in Cancer Research and Blick Scholar. To whom correspondence should be addressed: Dept. of Human and Molecular Genetics, Virginia Commonwealth University, 1220 East Broad St., P. O. Box 980035, Richmond, VA 23298. Tel.: 804-827-2339; Fax: 804-628-1176; E-mail: devanand.sarkar@vcuhealth.org.

[4] The abbreviations used are: HCC, hepatocellular carcinoma; MGLL, monoglyceride lipase; AT1R, angiotensin II type 1 receptor; Myr-Akt, myristoylated Akt; PIP3, phosphatidylinositol (3,4,5)-trisphosphate; Q-RT, quantitative RT; SN, staphylococcal nuclease; m, mouse; hHep, human hepatocyte; IP, immunoprecipitation; IB, immunoblot; IF, immunofluorescence; TCGA, the Cancer Genome Atlas; PCNA, proliferating cell nuclear antigen; MTT, 3-(4,5-dimethylthiazol-2-yl)-2,5-diphenyltetrazolium bromide; TD, tudor.

monoacylglycerol into glycerol and free fatty acids. Additionally, MGLL breaks down 2-arachidonoyl glycerol, the endogenous ligand for cannabinoid receptors, and thus negatively regulates endocannabinoid signaling (12). Because MGLL generates free fatty acids that might be utilized by cells as an energy source, one would anticipate that MGLL might promote tumorigenesis. However, there are conflicting reports regarding the role of MGLL in carcinogenesis. MGLL has been shown to be overexpressed in multiple tumor types, such as melanoma, ovarian, breast, and prostate cancers, positively regulating tumorigenesis (13). Conversely, studies in colon cancer show that MGLL is down-regulated and might function as a tumor suppressor (14). These discrepant findings indicate that MGLL might have organ-specific functions, and it might have expanded functions beyond its role as a lipid-metabolizing enzyme. Indeed, it has been demonstrated that MGLL selectively interacts with phosphatidic acid and phosphoinositide derivatives leading to inhibition of PI3K/Akt signaling, which might be a potential mechanism by which MGLL functions as a tumor suppressor (14).

In this study, we identified interaction between MGLL and SND1 that down-regulates MGLL. MGLL levels were significantly decreased in human HCC cells *versus* normal hepatocytes and in human HCC patients *versus* normal liver. Forced overexpression of MGLL in SND1-overexpressing HCC cells inhibited *in vitro* proliferation and *in vivo* tumorigenesis in nude mouse xenograft models. These findings uncover a novel molecular mechanism of SND1 action and define a unique tumor suppressor function of MGLL in HCC.

## Materials and Methods

*Plasmids*—FLAG-tagged expression constructs for full-length SND1 and SN and tudor domains of SND1 were kindly provided by Dr. Kirsi Paukku, University of Helsinki. The FLAG-Myc-tagged SND1 expression construct was obtained from Origene. Human MGLL cDNA was obtained from Origene and used as template to include a C-terminal HA tag by PCR using the following primers: sense, 5′-gctagcgccaccatgccagaggaaagttccccc-3′, and antisense, 5′-ggatcctcaagcgtaatctggaacatcgtatgggtagggtggggacgcagttcc-3′, and subcloned into NheI and BamHI sites of pcDNA3.1(+)-Hygro (pcDNA-MGLL-HA). This construct was used as template to generate the MGLLS122A mutant construct using QuikChange II XL site-directed mutagenesis kit (Agilent Technologies) and the primers sense, 5′- cttccttctgggccac**g**ccatgggaggcgccatc-3′, and antisense, 5′-gatggcgcctcccatgg**c**gtggcccagaaggaag-3′ (the mutated base is in bold), according to the manufacturer's instruction. Constitutively active Myr-Akt expression construct was kindly provided by Dr. Kristoffer Valerie, Virginia Commonwealth University.

*Cell Lines, Culture Condition, Proliferation, Viability, Clonogenicity, and Migration Assays*—Primary human hepatocytes were obtained from the Liver Tissue Cell Distribution System (National Institutes of Health contract N01-DK-7–0004/HHSN267200700004C) and cultured as described (15). Primary mouse hepatocytes were isolated from C57BL/6 mice and cultured as described (15). Hep3B cells were obtained from the American Type Culture Collection (Manassas, VA); QGY-7703 cells were obtained from Fudan University, China; and HepG3 and Huh7 cells were kindly provided by Dr. Paul Dent and cultured as described (16). Generation and characterization of control and SND1 shRNA expressing clones in QGY-7703 cells and SND1-overexpressing clone (Hep-SND1-17) in Hep3B cells have been described previously (2, 7, 8). MGLL-overexpressing stable clones of QGY-7703 and Hep-SND1-17 were generated by transfection of pcDNA-MGLL-HA plasmid, and independent clones were selected in the presence of 250 $\mu$g/ml hygromycin. Cell proliferation was determined by standard MTT assays as described (16). For QGY-7703 cells and its derived clones, 1000 cells/well were plated, and for Hep-SND1-17 cells and its derived clones, 2,000 cells/well were plated in a 96-well plate. For colony formation assay, cells (500) were plated in 6-cm dishes, and colonies of $>$50 cells were counted after 2 weeks (16). Cell viability was determined by trypan blue exclusion assay. Cell migration was analyzed by wound healing assay as described (7).

*Cell Cycle and Apoptosis Assays*—Cells were synchronized by double thymidine block essentially as described previously followed by release at 0 h (17). At the end of the experiment cells were harvested, fixed in 70% ethanol, and stained with propidium iodide followed by flow cytometry for cell cycle analysis. Apoptosis in cultured cells was determined by annexin V binding assay followed by flow cytometry and in tumor sections by TUNEL staining as described (17).

*Tissue Microarray and Immunostaining*—Human HCC tissue microarrays were obtained from Imgenex Corp. Two tissue microarrays were used as follows: one containing 40 primary HCC, 10 metastatic HCC, and 9 normal adjacent liver samples (Imgenex; IMH-360); and the other containing 46 primary HCC and 13 metastatic HCC (Imgenex; IMH-318). Immunostaining was performed using anti-SND1 antibody (rabbit polyclonal; 1:100; Prestige Antibodies® powered by Atlas antibodies from Sigma), anti-MGLL antibody (goat polyclonal; 1:250; Abcam), and anti-PCNA antibody (mouse monoclonal; 1:300; Cell Signaling) as described (16).

*Analysis of the Cancer Genome Atlas (TCGA) Database*—Level 3 gene expression data in different cancers were downloaded from TCGA using the TCGA2STAT R package (Version 1.2) (18). The gene expression data were provided as RNA-Seq by expectation-maximization values of 20,531 genes (19). The data were accessed on February 14, 2016. Genes positively/negatively correlated with SND1 were selected using Pearson's correlation coefficient (Hmisc::rcorr function) at $p$ value $<$0.01. The results presented here are in part based upon data generated by the TCGA Research Network at cancergenome.nih.gov.

*Co-immunoprecipitation (co-IP), Western Blot, and Immunofluorescence (IF) Analyses*—Co-IP and Western blot were performed as described (20). QGY-7703 cells were transfected with SND1-FLAG-Myc and MGLL-HA constructs. Immunoprecipitation (IP) was performed by anti-Myc antibody, and immunoblotting (IB) was performed by anti-HA antibody and vice versa. In a second experiment, QGY-7703 cells were transfected with FLAG-tagged full-length SND1 and its SN and tudor domain expression constructs and MGLL-HA construct. IP was performed with anti-FLAG antibody, and IB was performed by anti-HA antibody and vice versa. The primary anti-

bodies used for Western blot analysis are as follows: Cell Signaling: Akt, p-Akt (Thr-308), ERK, p-ERK, GSK3$\beta$, p-GSK3$\beta$, and ubiquitin (all rabbit; 1:1000); Sigma: SND1 and FLAG (rabbit; 1:1000); MGLL (ThermoFisher; rabbit; 1:1000); EF1$\alpha$ (Millipore; mouse; 1:1000); HA (Covance; mouse; 1:1000). For IF, QGY-7703 cells were transfected with SND1-FLAG-Myc and MGLL-HA constructs, and double IF was performed using anti-FLAG and anti-HA antibodies (2). Additionally, double IF was performed in primary mouse hepatocytes using anti-SND1 and anti-MGLL antibodies. The slides were analyzed by a confocal laser scanning microscope (Zeiss).

*Total RNA Expression and Q-RT-PCR*—Total RNA was extracted using Qiagen miRNeasy mini kit (Qiagen, Hilden, Germany). cDNA preparation was done using ABI cDNA synthesis kit. Real time-polymerase chain reaction (RT-PCR) was performed using an ABI ViiA7 fast real time PCR system and TaqMan gene expression assays according to the manufacturer's protocol (Applied Biosystems, Foster City, CA).

*MGLL Enzyme Activity Assay*—MGLL enzyme activity was measured in cell lysates using monoacylglycerol lipase inhibitor screening assay kit (Cayman Chemical, Ann Arbor, MI) according to the manufacturer's protocol. MGLL hydrolyzes 4-nitrophenylacetate to a yellow product 4-nitrophenol that can be measured at an absorbance of 405–412 nm.

*Nude Mice Xenograft Studies*—Subcutaneous xenografts were established in flanks of athymic nude mice using control and MGLL-overexpressing clones of QGY-7703 cells ($5 \times 10^5$) and control and MGLL-overexpressing clones of Hep-SND1-17 cells ($1 \times 10^6$) (2). Tumor volume was measured twice weekly with a caliper and calculated using the formula $\pi/6 \times$ larger diameter $\times$ (smaller diameter)$^2$. All experiments were performed with 6–8 mice in each group.

*Yeast Two-hybrid Assay*—Yeast two-hybrid assay was performed by DUAL hunter screening approach by Dual Systems Biotech AG (Schlieren, Switzerland) using SND1 as bait and human liver cDNA library as prey according to the methodology previously described (21).

## Results

SND1 interacts with proteins in diverse complexes to exert its function. To identify novel SND1-interacting proteins, we performed a modified yeast two-hybrid assay designed for transcriptionally active proteins that detect protein interaction outside of the nucleus (21). This strategy was utilized because SND1 functions as a coactivator for multiple transcription factors (22, 23). SND1 (the bait) was inserted between the membrane protein Ost4p and the C-terminal half of ubiquitin (Cub) followed by the artificial transcription factor LexA-VP16 (Fig. 1*A*). Human adult liver cDNA library (the prey) was fused with mutated N-terminal half of ubiquitin (NubG). Upon bait and prey interaction, Cub and NubG complement to form split-ubiquitin, followed by cleavage and translocation of LexA-VP16 to the nucleus and transcriptional activation of endogenous reporter genes, which is detected by growth selection on minimal medium. A total of 30 potential SND1-interacting proteins were identified (supplemental Table S1). We focused on MGLL because it showed in-frame screen-specific interaction with a highly significant *p* value; it has been indicated as either a tumor suppressor or tumor promoter in other cancers, and its role in SND1 function as well as in hepatocarcinogenesis has not been identified.

To confirm the SND1/MGLL interaction, we performed co-IP assay upon overexpression of FLAG-Myc-tagged SND1 and HA-tagged MGLL expression constructs in the human HCC cell line QGY-7703. IP with anti-Myc antibody followed by Western blot with anti-HA antibody and vice versa confirmed SND1/MGLL interaction (Fig. 1*B*). These transfected QGY-7703 cells were also subjected to double IF analysis using anti-FLAG (for SND1) and anti-HA (for MGLL) antibodies, and the merged image clearly shows co-localization of the two proteins indicating interaction between them (Fig. 1*C*). To further confirm endogenous interaction between SND1 and MGLL, double IF was performed in primary mouse hepatocytes using anti-SND1 and anti-MGLL antibodies, and the merged image shows co-localization of the two proteins (Fig. 1*D*).

We next checked which domain of SND1 interacts with MGLL. The N terminus of SND1 contains four tandem repeats of staphylococcal nuclease (SN) domains, and the C terminus contains a small tudor (TD) domain fused with a partial SN domain (Fig. 1*E*) (24). SN1–SN4 domains are involved in RNA binding; SN3–SN4 domains harbor the nuclease activity, and the TD domain facilitates protein/protein interaction (24, 25). FLAG-tagged expression constructs for full-length SND1 (SND1-FL), SN domains (SND1-SN), or tudor domain (SND1-TD) were transfected into QGY-7703 cells along with MGLL-HA construct and IP was performed using anti-FLAG antibody, and Western blot was performed using anti-HA antibody and vice versa. Interaction of MGLL was detected with SND1-FL and SND-SN but not with SND1-TD indicating that the SN domains of SND1 interact with MGLL (Fig. 1*F*).

We checked MGLL and SND1 protein levels in normal human hepatocytes (hHep) and mouse liver (mLiver) and human HCC cell lines QGY-7703, HuH-7, Hep3B, and HepG3 (Fig. 2*A*). Although MGLL expression was detected in hHep and mLiver, it could not be detected in any of the HCC cells. In reverse correlation, SND1 protein levels were substantially high in human HCC cells when compared with hHep and mLiver (Fig. 2*A*). Compared with hHep, human HCC cells expressed a significantly lower level of MGLL mRNA, which was still within the detection level of Q-RT-PCR (mean $CT < 30$ cycles) (Fig. 2*B*). However, the MGLL protein could not be detected in HCC cells even upon overexposure of the radiographic film suggesting that the MGLL protein level might be regulated at the level of translation or post-translation. Analysis of MGLL by immunohistochemistry in human tissue microarray revealed the high expression level in normal liver with progressive decrease along the stages of HCC (Fig. 2*C*). We previously analyzed expression of SND1 by immunohistochemistry in the same tissue microarray (2) and compared MGLL and SND1 expression levels. A significant negative correlation was observed between SND1 and MGLL protein levels with the stages of HCC (Fig. 2*D* and Table 1). We mined TCGA databases for all cancers to check negative correlation between SND1 and MGLL mRNA levels considering the *p* value of $<0.01$ as significant. A significant negative correlation between SND1 and MGLL mRNA levels was identified in cancers of breast, brain, colon, liver, lung,

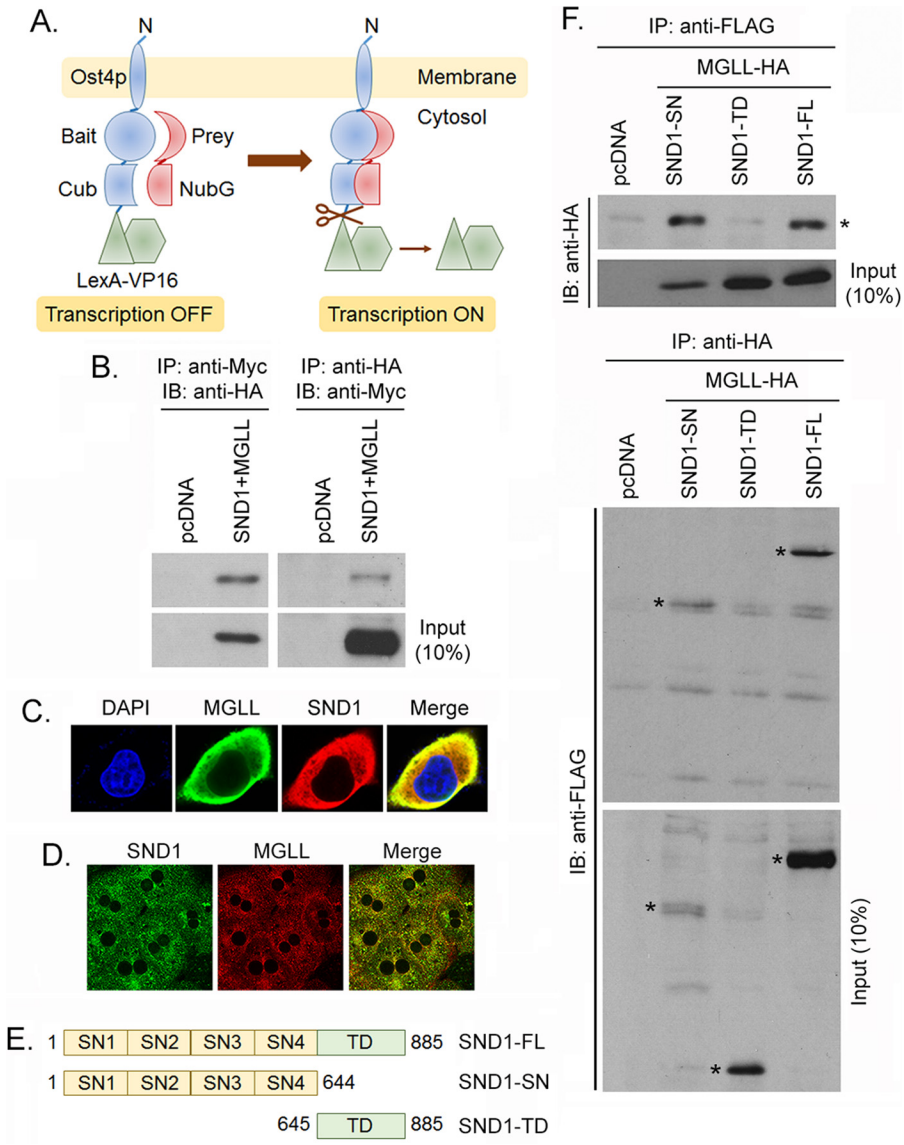


FIGURE 1. **SND1 and MGLL interact with each other.** *A,* schematic representation of the strategy of yeast two-hybrid assay. SND1 fused with Cub was used as bait, and NubG-fused adult human liver cDNA library was used as prey. *B,* QGY-7703 cells were transfected with FLAG-Myc-tagged SND1 and HA-tagged MGLL expression constructs. IP was performed using anti-Myc antibody, and IB was performed using anti-HA antibody and vice versa. *C,* QGY-7703 cells were transfected as in *B,* and double IF analysis was performed using anti-HA (for MGLL) and anti-FLAG (for SND1) antibodies. *D,* double IF analysis was performed in primary mouse hepatocytes using anti-SND1 and anti-MGLL antibodies. *E,* domain structure of full-length SND1 (SND1-FL) and its SN (SND1-SN) and tudor (SND1-TD) domains. *F,* SN domain of SND1 interact with MGLL. QGY-7703 cells were transfected with empty vector or expression constructs for FLAG-tagged SND1-SN, SND1-TD, and SND1-FL and HA-tagged MGLL. IP was performed using anti-FLAG antibody, and IB was performed using anti-HA antibody and vice versa. The *asterisks* represent specific bands.

prostate, and rectum (Table 2). Only renal cancers showed significant positive correlation.

We previously established and characterized stable clones of QGY-7703 cells expressing SND1 shRNA (shSND1-2 and shSND1-3) (2, 7, 8). Knocking down SND1 in these clones resulted in a detectable increase in MGLL protein level when compared with the control shRNA-expressing clone (shCon) (Fig. 2*E*). However, no difference in MGLL mRNA level was detected in shCon *versus* shSND1 clones (Fig. 2*F*). These findings suggest that interaction of SND1 with MGLL might interfere with MGLL protein turnover. MGLL enzyme activity level correlated with protein level in these cells (Fig. 2*G*).

We next checked potential regulation of MGLL protein turnover by SND1 by overexpressing them in Hep3B cells and treating the cells with proteasome inhibitor MG132 (5 $\mu$M). MG132 treatment substantially increased the MGLL level (compare *5th* and *6th lanes*) suggesting significant turnover of MGLL protein under basal conditions (Fig. 2*H*). Overexpression of SND1 significantly reduced MGLL level (compare *5th* and *7th lanes*), which was restored close to the basal level upon MG132 treatment (compare *5th* and *8th lanes*). MGLL overexpression did not affect SND1 levels (Fig. 2*H*).

We previously established and characterized stable clones of Hep3B cells expressing SND1 (Hep-SND1-17) to confirm the oncogenic properties of SND1 (2, 7, 8). Hep-SND1-17 cells were transfected with MGLL-HA construct, treated with MG132, and then IP was carried out using control IgG or anti-ubiquitin antibody, and IB was performed using anti-HA anti-

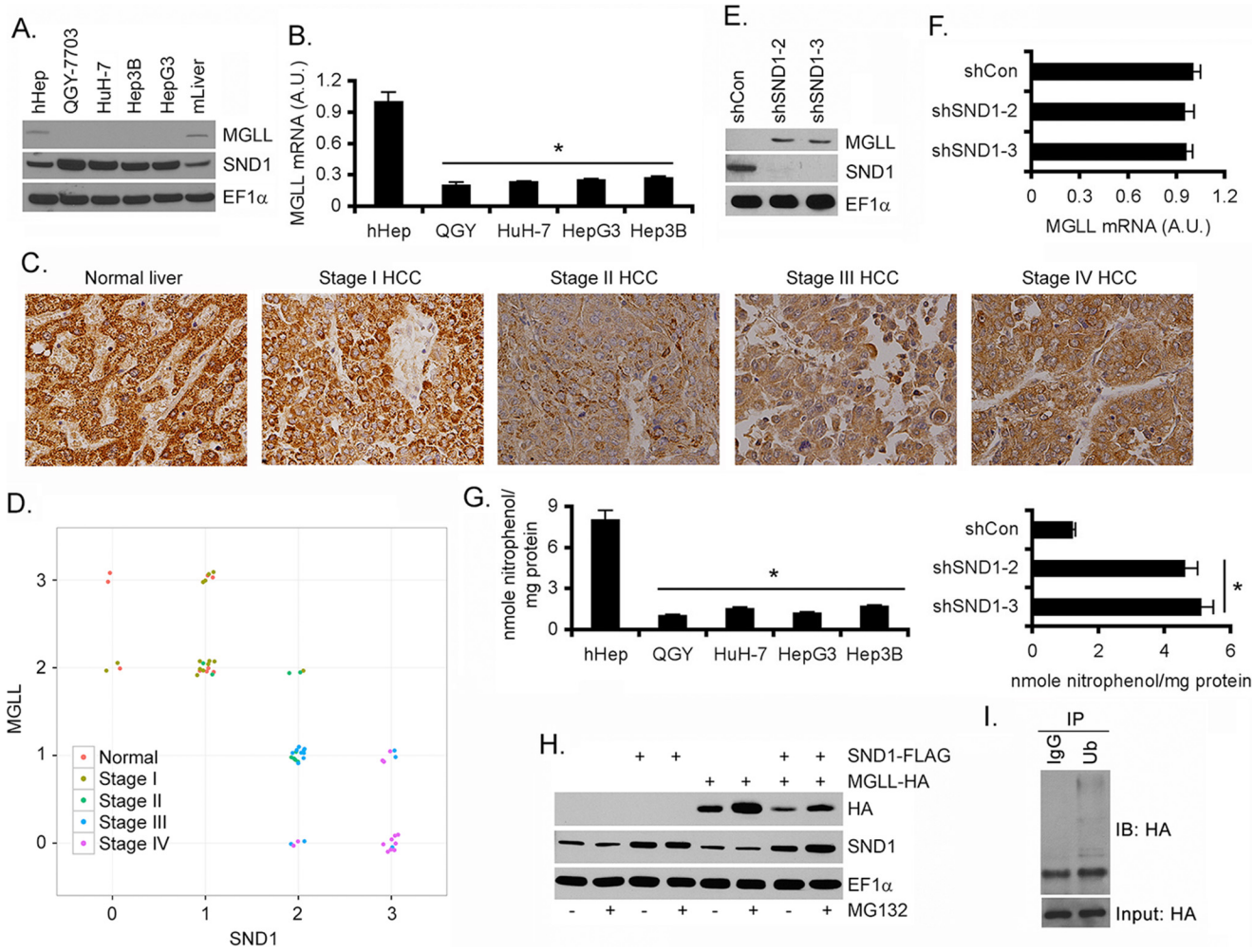


FIGURE 2. **MGLL is down-regulated in human HCC.** *A,* Western blot analysis for MGLL and SND1 in primary human hepatocytes (*hHep*), mouse liver (*mLiver*), and the indicated human HCC cell lines. EF1$\alpha$ was used as loading control. *B,* MGLL mRNA expression was analyzed by TaqMan Q-RT-PCR in the indicated cells. GAPDH was used for normalization. Normalized MGLL expression level in hHep was considered as 1. *A.U.,* arbitrary units. *C,* immunohistochemical analysis of MGLL in normal liver and different stages of HCC using a tissue microarray. *D,* to assess the strength of association between SND1 and MGLL, an ordinal logistic regression was conducted. Pearson's $\chi^2$ goodness of fit test with 6 degrees of freedom was performed. *p* value, $1.389 \times 10^{-13}$. *E,* Western blot analysis for MGLL and SND1 in stable clones of QGY-7703 cells expressing control shRNA (*shCon*) or SND1 shRNA (*shSND1–2* and *shSND1–3*). EF1$\alpha$ was used as loading control. *F,* MGLL mRNA expression was analyzed by TaqMan Q-RT-PCR in the indicated cells. GAPDH was used for normalization. *G,* MGLL enzymatic activity was analyzed in the indicated cells. *H,* Hep3B cells were transfected with MGLL-HA and SND1-FLAG-Myc constructs, alone or in combination, and 24 h after transfection, the cells were treated or not with MG132 (5 $\mu$M) for 12 h. Western blot analysis was performed using the indicated antibodies. *I,* Hep-SND1-17 cells were transfected with MGLL-HA, and 24 h after transfection, the cells were treated or not with MG132 (5 $\mu$M) for 12 h. IP was performed using control IgG and anti-ubiquitin antibody, and IB was performed using anti-HA antibody. For all the graphs, the data represent mean ± S.E. for three independent experiments. *, $p < 0.01$.

**TABLE 1**

**Cross-tabulation of SND1 and MGLL expression**

Pearson's $\chi^2$ test was used. The following data were used: *ct* $\chi^2 = 84.2027$; degrees of freedom = 6; *p* value, $1.389 \times 10^{-13}$.

| | 0 | 1 | 2 | 3 |
|---|---|---|---|---|
| 0 | 0.00 | 0.00 | 4.00 | 9.00 |
| 1 | 0.00 | 0.00 | 14.00 | 5.00 |
| 2 | 3.00 | 13.00 | 3.00 | 0.00 |
| 3 | 2.00 | 6.00 | 0.00 | 0.00 |

body. Ubiquitinated MGLL was detected upon IP with anti-ubiquitin antibody indicating that SND1 causes ubiquitination and proteasomal degradation of MGLL (Fig. 2*I*).

We established stable clones of QGY-7703 cells overexpressing MGLL (Fig. 3*A*). Compared with parental QGY-7703 cells and control clone (Con-1), MGLL overexpressing clones (MG-8B and MG-13B) showed marked reduction in proliferation as assayed by MTT and colony formation assays (Fig. 3, *B* and *C*). These clones also showed significant inhibition in cell migration analyzed by the wound healing assay (Fig. 3*D*). To decipher the mechanism of reduced proliferation following MGLL overexpression, we synchronized these clones by double thymidine block and then allowed them to continue through the cell cycle by removal of the high concentration of thymidine that inhibits ribonucleotide reductase. At 0 h, all the clones were predominantly in early S-phase indicating the efficacy of double thymidine block (Fig. 3*E*). However, the Con-1 clone completed the S-phase and progressed to $G_2$/M-phase significantly faster than MG-8B and MG-13B clones. At 4–6 h, a large percentage of Con-1 cells has completed the S-phase and entered into $G_2$/M-phase, although a significant percentage of MG-8B and MG-13B cells was still in the S-phase. At 10–12 h, the majority of the Con-1 cells has completed the cell cycle and

**TABLE 2**

**Correlation between SND1 and MGLL mRNA levels in different cancers in TCGA database**

Correlation coefficient is Pearson's correlation coefficient; Boldface type indicates significant negative correlation. Italic type indicates significant positive correlation. $p < 0.01$ is considered as significant.

| Cancer name | Acronym | Correlation coefficient | *p* value |
|---|---|---|---|
| Adrenocortical carcinoma | ACC | −0.0285 | 0.803074 |
| Bladder urothelial carcinoma | BLCA | 0.057641 | 0.234605 |
| **Breast invasive carcinoma** | **BRCA** | **−0.15905** | **2.59E-08** |
| Cervical and endocervical cancers | CESC | 0.095583 | 0.093502 |
| Cholangiocarcinoma | CHOL | 0.089728 | 0.557766 |
| **Colon adenocarcinoma** | **COAD** | **−0.44625** | **0** |
| **Colorectal adenocarcinoma** | **COADREAD** | **-0.40934** | **0** |
| Diffuse large B-cell lymphoma | DLBC | −0.11856 | 0.673885 |
| Esophageal carcinoma | ESCA | −0.01293 | 0.85729 |
| Gliobastoma multiforme | GBM | −0.0302 | 0.699316 |
| **Glioma** | **GBMLGG** | **−0.17932** | **1.93E-06** |
| Head and neck squamous cell carcinoma | HNSC | −0.09406 | 0.02523 |
| Kidney chromophobe | KICH | 0.097031 | 0.3602 |
| *Renal clear cell carcinoma* | *KIRC* | *0.305295* | *1.55E-14* |
| *Renal papillary cell carcinoma* | *KIRP* | *0.153594* | *0.005672* |
| Acute myeloid leukemia | LAML | 0.061737 | 0.419724 |
| **Brain low grade glioma** | **LGG** | **−0.20584** | **1.76E-06** |
| **Hepatocellular carcinoma** | **LIHC** | **−0.20089** | **3.15E-05** |
| **Lung adenocarcinoma** | **LUAD** | **−0.1702** | **4.03E-05** |
| **Lung squamous cell carcinoma** | **LUSC** | **−0.1931** | **4.88E-06** |
| Mesothelioma | MESO | 0.006992 | 0.948755 |
| Ovarian serous cystadenocarcinoma | OV | 0.062941 | 0.271587 |
| Pancreatic adenocarcinoma | PAAD | −0.00038 | 0.995988 |
| Pheochromocytoma and paraganglioma | PCPG | 0.153765 | 0.035631 |
| **Prostate adenocarcinoma** | **PRAD** | **−0.16521** | **9.92E-05** |
| **Rectum adenocarcinoma** | **READ** | **−0.29397** | **0.002336** |
| Sarcoma | SARC | −0.0785 | 0.202749 |
| Skin cutaneous melanoma | SKCM | −0.04513 | 0.327329 |
| Stomach adenocarcinoma | STAD | −0.22576 | 0.155825 |
| Testicular germ cell tumors | TGCT | −0.15511 | 0.053172 |
| Thyroid carcinoma | THCA | 0.044937 | 0.285 |
| Thymoma | THYM | −0.21434 | 0.017754 |
| Uterine corpus endometrial carcinoma | UCEC | −0.01829 | 0.796627 |
| Uterine carcinosarcoma | UCS | −0.14564 | 0.279707 |
| Uveal melanoma | UVM | 0.09193 | 0.417351 |

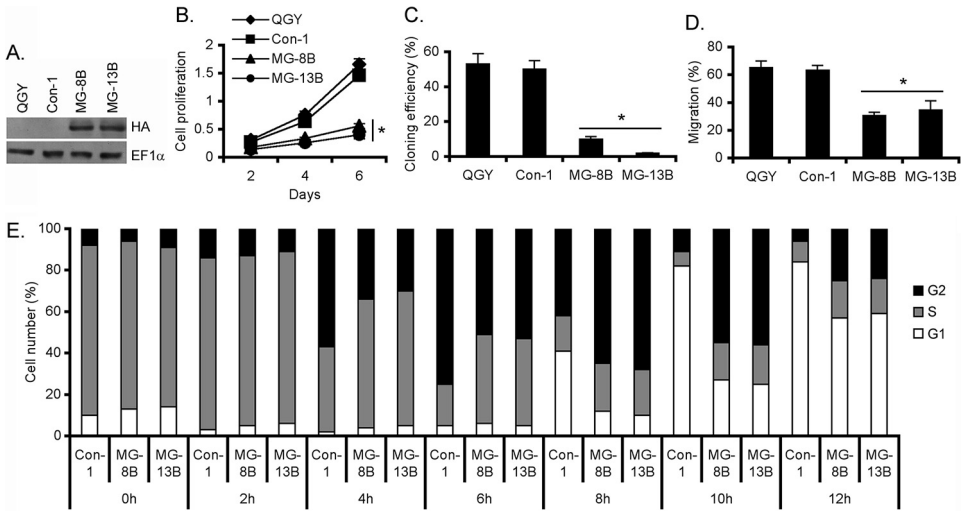


FIGURE 3. **Overexpression of MGLL inhibits proliferation and delays cell cycle progression in QGY-7703 cells.** *A,* Western blot analysis in parental QGY-7703 cells and its stable control clone (*Con-1*) and HA-tagged MGLL-expressing clones (*MG-8B* and *MG-13B*) using anti-HA antibody. EF1$\alpha$ was used as loading control. Cell proliferation (*B*), colony formation (*C*), and migration using wound healing assay (*D*) were analyzed in the indicated cells. *B–D,* data represent mean ± S.E. for three independent experiments. *, $p < 0.01$. *E,* indicated cells were synchronized at S-phase by double thymidine block, released in full media (0 h), and cell cycle was analyzed at the indicated time points. Graphical representation of percentage of cells in different phases of cell cycle is shown.

returned to $G_1$-phase although a significant percentage of MG-8B and MG-13B cells were still in the $G_2$/M-phase. Analysis of cell viability and apoptosis did not show any difference between these clones (data not shown) indicating that the reduced proliferation upon MGLL overexpression is predominantly due to delay in progression through cell cycle.

To check whether MGLL overexpression overrides SND1 function, we established stable clones of Hep-SND1-17 cells overexpressing MGLL (SND1-17-MG-2 and SND1-17-MG-9) (Fig. 4*A*). Similar to MGLL-overexpressing clones of QGY-7703 cells, SND1-17-MG-2 and SND1-17-MG-9 clones also showed reduced proliferation, migration, and delay in cell cycle

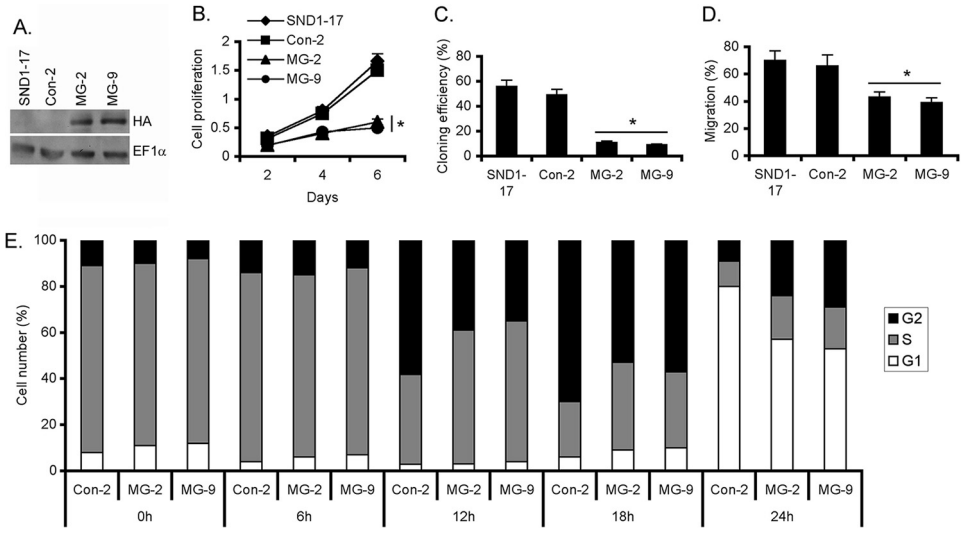


FIGURE 4. **Overexpression of MGLL inhibits proliferation and delays cell cycle progression in Hep-SND1-17.** *A,* Western blot analysis in parental Hep-SND1-17 cells (Hep3B cells stably overexpressing SND1) and its stable control clone (*Con-2*) and HA-tagged MGLL expressing clones (*MG-2* and *MG-9*) using anti-HA antibody. EF1$\alpha$ was used as loading control. Cell proliferation (*B*), colony formation (*C*) and migration using wound healing assay (*D*) were analyzed in the indicated cells. *B–D,* data represent mean ± S.E. for three independent experiments. *, $p < 0.01$. *E,* indicated cells were synchronized at S-phase by double thymidine block, released in full media (0 h), and cell cycle was analyzed at the indicated time points. Graphical representation of percentage of cells in different phases of cell cycle is shown.

progression compared with parental Hep-SND-17 cells and control clone (Hep-SND1-17-Con-2) (Fig. 4, *B–E*).

Previous studies showed that knocking down MGLL results in activation of Akt (14). We checked activation of Akt and its downstream signaling molecule GSK3$\beta$, ERK1/2 in control, and MGLL-overexpressing clones of QGY-7703 and Hep-SND1-17 cells. A profound inhibition in Akt and GSK3$\beta$ activation was observed upon MGLL overexpression (Fig. 5*A*). However, no significant change in the level of activated ERK1/2 was observed. However, knocking down SND1 in QGY-7703 cells resulted in inhibition of both Akt and ERK (Fig. 5*B*). To check the role of Akt inhibition in mediating the MGLL effect, we overexpressed a constitutively active Akt (Myr-Akt) (26) in MGLL-overexpressing clones and analyzed for cell proliferation and cell cycle progression. Myr-Akt significantly protected cells from the inhibitory effects of MGLL as evidenced by increased proliferation by MTT assay, increased clonogenic efficiency, and rescue from the delay in cell cycle progression (Fig. 5, *C–E*).

To check whether MGLL enzymatic activity is required for inhibition of Akt and cell proliferation, we created a mutant construct of MGLL. MGLL is a serine hydrolase containing the G*X*S*X*G consensus sequence in which the serine residue at amino acid 122 is critical for its catalytic activity (Fig. 6*A*) (27). We mutated this serine residue to alanine (MGLLS122A) and transiently overexpressed WT MGLL and MGLLS122A into QGY-7703 cells (Fig. 6*B*). MGLLS122A lost its enzymatic activity (Fig. 6*C*). However, it still effectively inhibited activation of Akt and cell proliferation as measured by MTT and colony formation assays (Fig. 6, *B, D,* and *E*, respectively).

The tumorigenic potential of cells upon overexpression of MGLL was checked by *in vivo* assays. MG-8B and MG-9B clones of QGY-7703 cells and MG-2 and MG-9 clones of Hep-SND1-17 cells showed profound inhibition of growth when implanted subcutaneously in athymic nude mice compared with their corresponding control clones (Fig. 7, *A* and *B*). Tumors derived from MGLL-overexpressing clones showed marked reduction in PCNA staining compared with the control clones (Fig. 7, *C* and *D*), although no significant difference in apoptosis was observed (data not shown) further indicating that interference with proliferation is the major mechanism by which MGLL overexpression reduces growth of human HCC cells.

## Discussion

In this study, we describe a novel mechanism by which SND1 promotes HCC. SND1 has been shown to interact with a diverse array of proteins thereby regulating fundamental cellular processes such as transcription, mRNA splicing, RNA editing, and miRNA function (1). This is the first documentation that SND1 also regulates gene function at a post-translational level. We demonstrate that interaction of SND1 with MGLL results in increased ubiquitination and subsequent proteosomal degradation of MGLL. This down-regulation of MGLL is required for SND1 to exert its pro-tumorigenic activity because forced overexpression of MGLL markedly abrogates cell proliferation. Our studies thereby unravel a novel tumor suppressor function of MGLL in the context of HCC. We document an inverse correlation between SND1 and MGLL levels with the progression of HCC, which confers clinical relevance to our findings. In HCC, the inverse correlation was much stronger at the level of protein ($p$ value $1.389 \times 10^{-13}$) *versus* at the level of mRNA ($p$ value $3.15 \times 10^{-5}$). Additionally, at the level of mRNA the inverse correlation was much stronger in colorectal carcinoma ($p$ value 0). These findings suggest that in HCC, MGLL down-regulation occurs predominantly at the protein level, which is mediated by its interaction with SND1.

Compared with human hepatocytes, a significant decrease in MGLL mRNA levels was detected in human HCC cell lines. Thus, apart from a post-translational regulation by

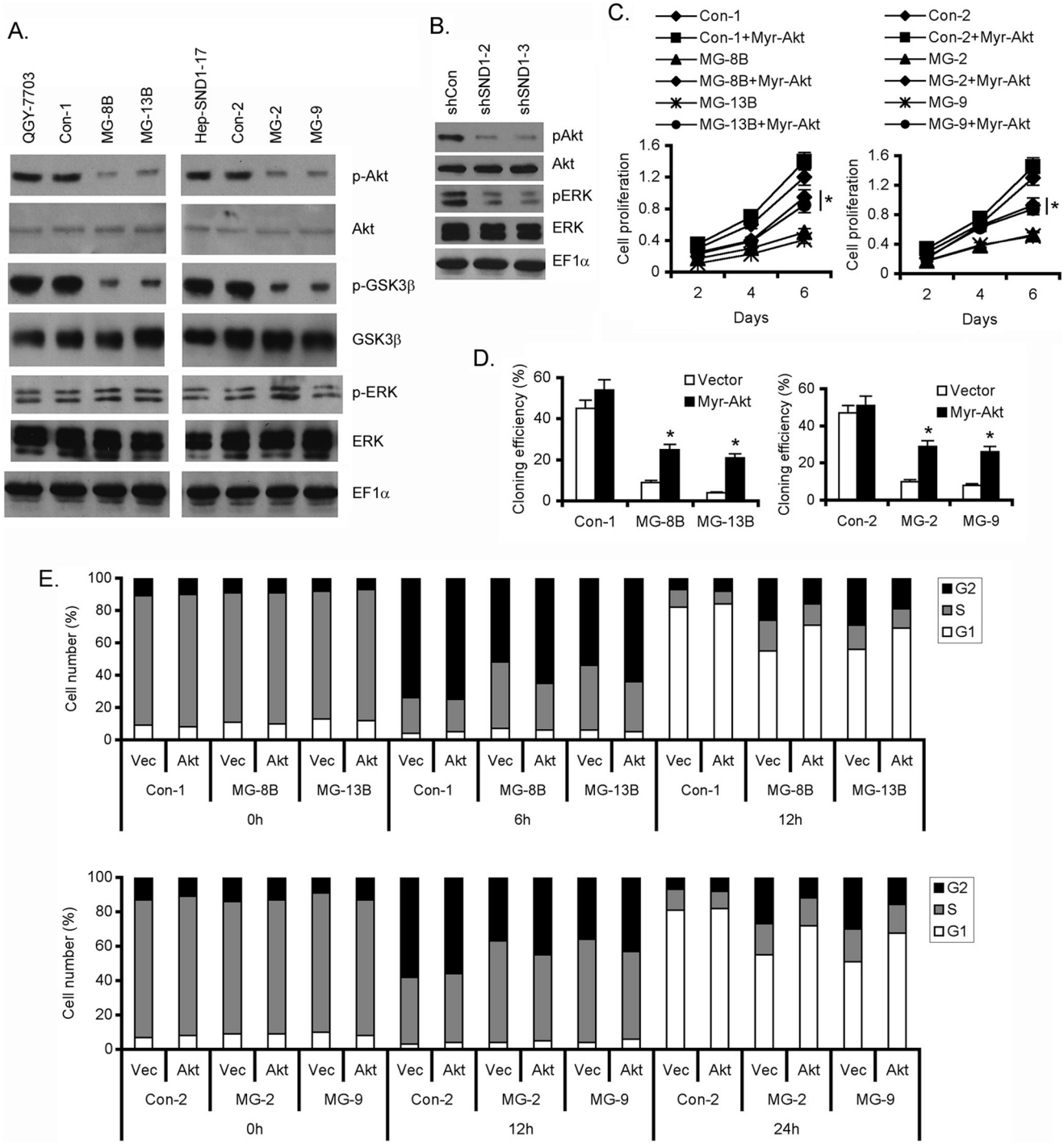


FIGURE 5. **MGLL overexpression inhibits Akt activation and constitutively active Akt protects from inhibitory effects of MGLL.** *A,* Western blot analysis of the indicated proteins in control (*Con-1*) and MGLL-HA-overexpressing clones (*MG-8B* and *MG-13B*) of QGY-7703 cells and control (*Con-2*) and MGLL-HA-overexpressing clones (*MG-2* and *MG-9*) of Hep-SND1-17 cells. *B,* Western blot analysis of the indicated proteins in stable clones of QGY-7703 cells expressing control shRNA (*shCon*) or SND1 shRNA (*shSND1–2* and *shSND1–3*). EF1α was used as loading control. *C–E,* indicated cells were transfected with an expression construct for constitutively active Akt (*Myr-Akt*). Cell proliferation (*C*), colony formation (*D*), and cell cycle (*E*) analyses were performed. *C–E,* data represent mean ± S.E. for three independent experiments. *, $p < 0.01$. *E*, cells were synchronized by double thymidine block, and the panels show graphical representation of percentage of cells in different phases of cell cycle.

SND1, there is a regulation of MGLL at a transcriptional/post-transcriptional level leading to its down-regulation in HCC patients. MGLL is localized in human chromosome 3q21.3. Array comparative genomic hybridization analyses have shown less frequent changes in 3q in HCC patients with reports of both gains and losses at a low frequency (28, 29). Thus, deletion or loss-of-heterozygosity may not underlie MGLL down-regulation in HCC patients. The mechanism by which MGLL mRNA is down-regulated in HCC cells remains to be determined, and in-depth studies on the regulation of MGLL expression needs to be performed. However, the observation that MGLL is down-regulated both at

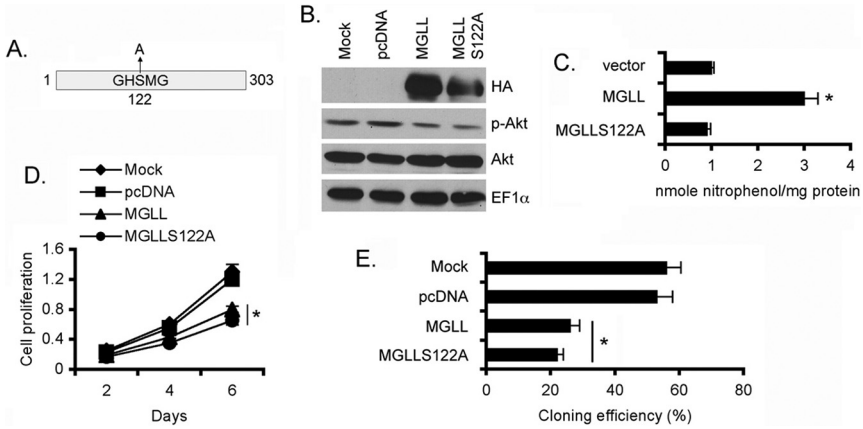


FIGURE 6. **MGLL enzymatic activity is not necessary for inhibition of Akt and cell growth.** *A,* schematic structure of MGLL protein showing G*X*S*X*G motif in which serine 122 was mutated to alanine. *B–E,* QGY-7703 cells were transiently transfected with empty vector (pcDNA3.1), WT MGLL, or MGLLS122A expression constructs. Western blot analysis of the indicated proteins is shown (*B*). EF1$\alpha$ was used as loading control. MGLL enzymatic activity was measured (*C*). MTT (*D*) and colony formation (*E*) assays were performed. For graphs, the data represent mean ± S.E. for three independent experiments. *, $p < 0.01$.

mRNA and protein levels suggests that MGLL might have a critical role in tightly regulating homeostatic proliferation of hepatocytes, and MGLL down-regulation is a prerequisite for a transformed cell to progress faster through the cell cycle and proliferate rapidly. Overexpression of MGLL results in a significant delay in progression through the cell cycle further supporting this hypothesis.

The major consequence of overexpression of MGLL is a profound inhibition in activation of Akt signaling, which is independent of its enzymatic activity. MGLL has been shown to bind to phosphatidylinositol (3,4,5)-trisphosphate (PIP3) (14), which is generated from phosphatidylinositol (4,5)-bisphosphate (PIP2) by phosphatidylinositol 3-kinase (PI3K). Akt and PDK1 bind to PIP3 at the plasma membrane, and PDK1 phosphorylates the activation loop of Akt at Thr-308 (30). The phosphatase and tensin homolog (PTEN) dephosphorylates PIP3 to phosphatidylinositol 4,5-bisphosphate and thus prevents Akt activation. Activation of PI3K/Akt signaling is a common event in HCC, and PTEN inactivation is frequently observed in human HCC patients (31). MGLL down-regulation provides another level of regulation for robust activation of PI3K/Akt signaling. Activation of Akt promotes cell proliferation, migration, invasion, and metastasis. Indeed, we observe that overexpression of MGLL not only encumbers proliferation, it also mitigates migration of human HCC cells. However, the inhibitory effect on proliferation was substantially more robust than that on migration. Overexpression of a constitutively active Akt significantly protected from the inhibitory effects of MGLL indicating an essential role of Akt inhibition in mediating MGLL function. MGLL overexpression did not affect ERK phosphorylation, although knocking down SND1 resulted in inhibition of both Akt and ERK activation. We previously documented that SND1 increases the AT1R level by increasing AT1R mRNA stability resulting in activation of ERK (7). Accordingly, SND1 might activate ERK axis via AT1R and Akt axis via inhibition of MGLL. One limitation of this study is that we could not analyze the effect of MGLL knockdown because MGLL cannot be detected at the protein level in human HCC cells. An MGLL knock-out mouse has been generated and characterized for behavioral response (32). This model would be ideal to further characterize tumor suppressor properties of MGLL.

Although Tudor domains are known to provide interface for protein/protein interactions (33), we identified that SN domains, not TD domain, of SND1 interact with MGLL. SN domains confer enzymatic activity and RNA binding. However, these domains have been shown to interact with other proteins. Interaction of SN1-SN2 domains of SND1 with the oncogene AEG-1/MTDH is necessary to protect SND1 from stress-induced degradation and mediate its oncogenic function (25). Our studies document that interaction of SND1 with MGLL results in MGLL degradation without affecting SND1 documenting the versatility of SND1 function.

Interaction of SND1 and MGLL might facilitate recruitment of an E3 ubiquitin ligase promoting MGLL ubiquitination and degradation. As yet, the particular E3 ubiquitin ligase mediating MGLL ubiquitination remains to be determined. In the TCGA breast cancer database, E3 ubiquitin ligase Smurf1 has been shown to positively correlate (Pearson's correlation coefficient = 0.5) with SND1, and SND1 has been shown to induce expression of Smurf1, which ubiquitinates and targets RhoA for destruction (9). However, whether SND1, Smurf1, and RhoA interact with each other in a complex has not been shown. Our analysis of TCGA HCC and colorectal cancer databases did not identify a strong positive correlation between Smurf1 and SND1, in both cases Pearson's correlation coefficient value was ~0.2. Hence, SND1-correlating genes might be different between breast cancer and gastrointestinal cancers, and further studies need to be carried out to identify MGLL targeting E3 ubiquitin ligase that might interact with SND1.

In summary, we identify a distinctive role of MGLL functioning as a tumor suppressor for HCC. MGLL overexpression profoundly inhibited cell proliferation without inducing cell death. Consequently, liver-targeted delivery of MGLL as a single modality may not be a viable and therapeutic option for HCC that would provide a lasting effect. However, it

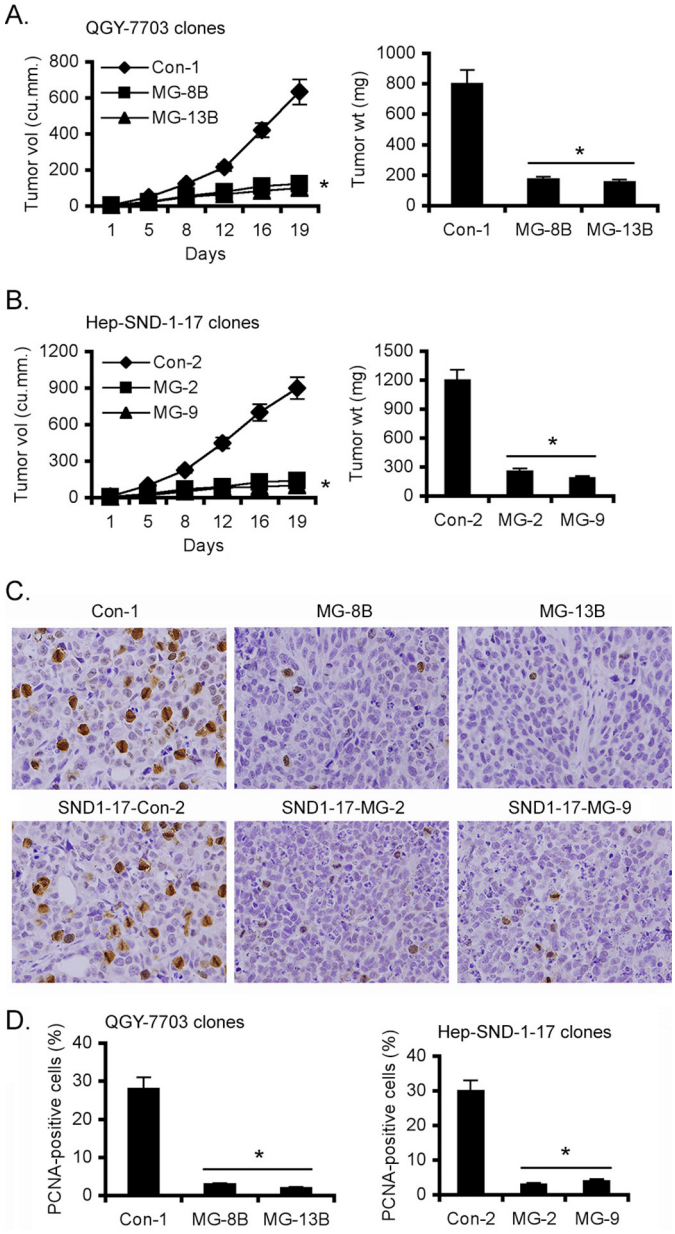


FIGURE 7. **Tumor formation by MGLL-overexpressing clones is markedly inhibited with abrogation of proliferation.** *A,* control (*Con-1*) and MGLL-HA-overexpressing clones (*MG-8B* and *MG-13B*) of QGY-7703 cells ($5 \times 10^5$) were subcutaneously implanted in athymic nude mice, and tumor volume (*left panel*) was measured to monitor tumor growth, and tumor weight (*right panel*) was measured at the end of the study. *B,* control (*Con-2*) and MGLL-HA-overexpressing clones (*MG-2* and *MG-9*) of Hep-SND1-17 cells ($1 \times 10^6$) were subcutaneously implanted in athymic nude mice, and tumor volume (*left panel*) was measured to monitor tumor growth, and tumor weight (*right panel*) was measured at the end of the study. *C,* immunohistochemical staining for PCNA in the indicated tumor samples. *D,* quantification of PCNA-positive cells in the tumor samples. *A, B,* and *D*, data represent mean ± S.E. for three independent experiments. *, $p < 0.01$.

might be considered as an adjuvant in a combinatorial treatment strategy.

*Author Contributions*—D. R. designed, performed, analyzed the experiments, and wrote the paper. N. J., R. G. M., C. L. R., M. A. A., and M. D. performed the experiments and the analyzed data. P. B. F. wrote the paper. D. S. conceived and coordinated the study, performed the experiments, analyzed the data, and wrote the paper.

## References


1. Jariwala, N., Rajasekaran, D., Srivastava, J., Gredler, R., Akiel, M. A., Robertson, C. L., Emdad, L., Fisher, P. B., and Sarkar, D. (2015) Role of the staphylococcal nuclease and tudor domain containing 1 in oncogenesis (review). *Int. J. Oncol.* **46,** 465–473
2. Yoo, B. K., Santhekadur, P. K., Gredler, R., Chen, D., Emdad, L., Bhutia, S., Pannell, L., Fisher, P. B., and Sarkar, D. (2011) Increased RNA-induced silencing complex (RISC) activity contributes to hepatocelllular carcinoma. *Hepatology* **53,** 1538–1548
3. Blanco, M. A., Alečković, M., Hua, Y., Li, T., Wei, Y., Xu, Z., Cristea, I. M., and Kang, Y. (2011) Identification of staphylococcal nuclease domain-containing 1 (SND1) as a Metadherin-interacting protein with metastasis-promoting functions. *J. Biol. Chem.* **286,** 19982–19992
4. Tsuchiya, N., Ochiai, M., Nakashima, K., Ubagai, T., Sugimura, T., and Nakagama, H. (2007) SND1, a component of RNA-induced silencing complex, is up-regulated in human colon cancers and implicated in early stage colon carcinogenesis. *Cancer Res.* **67,** 9568–9576
5. Kuruma, H., Kamata, Y., Takahashi, H., Igarashi, K., Kimura, T., Miki, K., Miki, J., Sasaki, H., Hayashi, N., and Egawa, S. (2009) Staphylococcal nuclease domain-containing protein 1 as a potential tissue marker for prostate cancer. *Am. J. Pathol.* **174,** 2044–2050
6. Wan, L., Lu, X., Yuan, S., Wei, Y., Guo, F., Shen, M., Yuan, M., Chakrabarti, R., Hua, Y., Smith, H. A., Blanco, M. A., Chekmareva, M., Wu, H., Bronson, R. T., Haffty, B. G., *et al.* (2014) MTDH-SND1 interaction is crucial for expansion and activity of tumor-initiating cells in diverse oncogene- and carcinogen-induced mammary tumors. *Cancer Cell* **26,** 92–105
7. Santhekadur, P. K., Akiel, M., Emdad, L., Gredler, R., Srivastava, J., Rajasekaran, D., Robertson, C. L., Mukhopadhyay, N. D., Fisher, P. B., and Sarkar, D. (2014) Staphylococcal nuclease domain containing-1 (SND1) promotes migration and invasion via angiotensin II type 1 receptor (AT1R) and TGF$\beta$ signaling. *FEBS Open Bio.* **4,** 353–361
8. Santhekadur, P. K., Das, S. K., Gredler, R., Chen, D., Srivastava, J., Robertson, C., Baldwin, A. S., Jr., Fisher, P. B., and Sarkar, D. (2012) Multifunction protein staphylococcal nuclease domain containing 1 (SND1) promotes tumor angiogenesis in human hepatocellular carcinoma through novel pathway that involves nuclear factor κB and miR-221. *J. Biol. Chem.* **287,** 13952–13958
9. Yu, L., Liu, X., Cui, K., Di, Y., Xin, L., Sun, X., Zhang, W., Yang, X., Wei, M., Yao, Z., and Yang, J. (2015) SND1 acts downstream of TGF$\beta$1 and upstream of Smurf1 to promote breast cancer metastasis. *Cancer Res.* **75,** 1275–1286
10. Sundström, J. F., Vaculova, A., Smertenko, A. P., Savenkov, E. I., Golovko, A., Minina, E., Tiwari, B. S., Rodriguez-Nieto, S., Zamyatnin, A. A., Jr., Välineva, T., Saarikettu, J., Frilander, M. J., Suarez, M. F., Zavialov, A., Ståhl, U., *et al.* (2009) Tudor staphylococcal nuclease is an evolutionarily conserved component of the programmed cell death degradome. *Nat. Cell Biol.* **11,** 1347–1354
11. Quiroga, A. D., and Lehner, R. (2012) Liver triacylglycerol lipases. *Biochim. Biophys. Acta* **1821,** 762–769
12. Dinh, T. P., Carpenter, D., Leslie, F. M., Freund, T. F., Katona, I., Sensi, S. L., Kathuria, S., and Piomelli, D. (2002) Brain monoglyceride lipase participating in endocannabinoid inactivation. *Proc. Natl. Acad. Sci. U.S.A.* **99,** 10819–10824
13. Nomura, D. K., Long, J. Z., Niessen, S., Hoover, H. S., Ng, S. W., and Cravatt, B. F. (2010) Monoacylglycerol lipase regulates a fatty acid network that promotes cancer pathogenesis. *Cell* **140,** 49–61
14. Sun, H., Jiang, L., Luo, X., Jin, W., He, Q., An, J., Lui, K., Shi, J., Rong, R., Su, W., Lucchesi, C., Liu, Y., Sheikh, M. S., and Huang, Y. (2013) Potential tumor-suppressive role of monoglyceride lipase in human colorectal cancer. *Oncogene* **32,** 234–241
15. Srivastava, J., Siddiq, A., Emdad, L., Santhekadur, P. K., Chen, D., Gredler, R., Shen, X.-N., Robertson, C. L., Dumur, C. I., Hylemon, P. B., Mukhopadhyay, N. D., Bhere, D., Shah, K., Ahmad, R., Giashuddin, S., *et al.* (2012) Astrocyte elevated gene-1 (AEG-1) promotes hepatocarcinogenesis: novel insights from a mouse model. *Hepatology* **56,** 1782–1791
16. Yoo, B. K., Emdad, L., Su, Z. Z., Villanueva, A., Chiang, D. Y., Mukhopadhyay, N. D., Mills, A. S., Waxman, S., Fisher, R. A., Llovet, J. M., Fisher,

P. B., and Sarkar, D. (2009) Astrocyte elevated gene-1 regulates hepatocellular carcinoma development and progression. *J. Clin. Invest.* **119,** 465–477
17. Rajasekaran, D., Siddiq, A., Willoughby, J. L., Biagi, J. M., Christadore, L. M., Yunes, S. A., Gredler, R., Jariwala, N., Robertson, C. L., Akiel, M. A., Shen, X.-N., Subler, M. A., Windle, J. J., Schaus, S. E., Fisher, P. B., *et al.* (2015) Small molecule inhibitors of late SV40 factor (LSF) abrogate hepatocellular carcinoma (HCC): evaluation using an endogenous HCC model. *Oncotarget* **6,** 26266–26277
18. Zhu, Y., Qiu, P., and Ji, Y. (2014) TCGA-assembler: open-source software for retrieving and processing TCGA data. *Nat. Methods* **11,** 599–600
19. Li, B., and Dewey, C. N. (2011) RSEM: accurate transcript quantification from RNA-Seq data with or without a reference genome. *BMC Bioinformatics* **12,** 323
20. Srivastava, J., Robertson, C. L., Rajasekaran, D., Gredler, R., Siddiq, A., Emdad, L., Mukhopadhyay, N. D., Ghosh, S., Hylemon, P. B., Gil, G., Shah, K., Bhere, D., Subler, M. A., Windle, J. J., Fisher, P. B., and Sarkar, D. (2014) AEG-1 regulates retinoid X receptor and inhibits retinoid signaling. *Cancer Res.* **74,** 4364–4377
21. Stagljar, I., Korostensky, C., Johnsson, N., and te Heesen, S. (1998) A genetic system based on split-ubiquitin for the analysis of interactions between membrane proteins *in vivo*. *Proc. Natl. Acad. Sci. U.S.A.* **95,** 5187–5192
22. Paukku, K., Yang, J., and Silvennoinen, O. (2003) Tudor and nuclease-like domains containing protein p100 function as coactivators for signal transducer and activator of transcription 5. *Mol. Endocrinol.* **17,** 1805–1814
23. Yang, J., Aittomäki, S., Pesu, M., Carter, K., Saarinen, J., Kalkkinen, N., Kieff, E., and Silvennoinen, O. (2002) Identification of p100 as a coactivator for STAT6 that bridges STAT6 with RNA polymerase II. *EMBO J.* **21,** 4950–4958
24. Li, C. L., Yang, W. Z., Chen, Y. P., and Yuan, H. S. (2008) Structural and functional insights into human Tudor-SN, a key component linking RNA interference and editing. *Nucleic Acids Res.* **36,** 3579–3589
25. Guo, F., Wan, L., Zheng, A., Stanevich, V., Wei, Y., Satyshur, K. A., Shen, M., Lee, W., Kang, Y., and Xing, Y. (2014) Structural insights into the tumor-promoting function of the MTDH-SND1 complex. *Cell Rep* **8,** 1704–1713
26. Jiang, B. H., Zheng, J. Z., Aoki, M., and Vogt, P. K. (2000) Phosphatidylinositol 3-kinase signaling mediates angiogenesis and expression of vascular endothelial growth factor in endothelial cells. *Proc. Natl. Acad. Sci. U.S.A.* **97,** 1749–1753
27. Labar, G., Bauvois, C., Borel, F., Ferrer, J. L., Wouters, J., and Lambert, D. M. (2010) Crystal structure of the human monoacylglycerol lipase, a key actor in endocannabinoid signaling. *Chembiochem* **11,** 218–227
28. Hashimoto, K., Mori, N., Tamesa, T., Okada, T., Kawauchi, S., Oga, A., Furuya, T., Tangoku, A., Oka, M., and Sasaki, K. (2004) Analysis of DNA copy number aberrations in hepatitis C virus-associated hepatocellular carcinomas by conventional CGH and array CGH. *Mod. Pathol.* **17,** 617–622
29. Patil, M. A., Gütgemann, I., Zhang, J., Ho, C., Cheung, S. T., Ginzinger, D., Li, R., Dykema, K. J., So, S., Fan, S. T., Kakar, S., Furge, K. A., Büttner, R., and Chen, X. (2005) Array-based comparative genomic hybridization reveals recurrent chromosomal aberrations and Jab1 as a potential target for 8q gain in hepatocellular carcinoma. *Carcinogenesis* **26,** 2050–2057
30. Manning, B. D., and Cantley, L. C. (2007) AKT/PKB signaling: navigating downstream. *Cell* **129,** 1261–1274
31. Villanueva, A., Newell, P., Chiang, D. Y., Friedman, S. L., and Llovet, J. M. (2007) Genomics and signaling pathways in hepatocellular carcinoma. *Semin. Liver Dis.* **27,** 55–76
32. Petrenko, A. B., Yamazaki, M., Sakimura, K., Kano, M., and Baba, H. (2014) Augmented tonic pain-related behavior in knockout mice lacking monoacylglycerol lipase, a major degrading enzyme for the endocannabinoid 2-arachidonoylglycerol. *Behav. Brain Res.* **271,** 51–58
33. Pek, J. W., Anand, A., and Kai, T. (2012) Tudor domain proteins in development. *Development* **139,** 2255–2266